ELSEVIER

Journal of Structural Geology 26 (2004) 2211–2224

JOURNAL OF STRUCTURAL GEOLOGY

www.elsevier.com/locate/jsg

Reference frame, angular momentum, and porphyroblast rotation

Dazhi Jiang[a,*], Paul F. Williams[b]

[a]Department of Geology, University of Maryland, College Park, MD 20742, USA
[b]Department of Geology, University of New Brunswick, P.O. Box 4400, Fredericton, NB, Canada E3B 5A3

Received 30 September 2003; received in revised form 24 June 2004; accepted 29 June 2004

Abstract

Rotation of small rigid objects in a deforming ductile matrix can produce two different types of microstructure: a shape fabric due to alignment of the principal axes of a population of elongate objects and the inclusion trail microstructure preserved in syntectonic porphyroblasts. We use numerical modeling to show that inclusion trails of elongate porphyroblasts are expected to be extremely complex. In contrast, snowball garnets are readily interpretable. But misuse of reference frame and kinematic misconceptions have obfuscated the discussion on the formation of porphyroblast inclusion trails in general and snowball garnet inclusion trails in particular. We clarify this point. Models for snowball garnet formation that are based on the notion of garnets being irrotational with respect to the earth can be rejected on a geometrical and kinematic basis. Further, the notion that rigid objects embedded in a deforming ductile matrix generally do not rotate is unsound—it violates the fundamental physical law of balance of angular momentum.

Keywords: Microstructure; Porphyroblast; Inclusion trail; Rotation; Snowball garnet; Vorticity

1. Introduction

Inclusion trails in porphyroblasts are common in metamorphic rocks. Although geologists have devoted a lot of effort to interpreting them, considerable controversy still exists even for simple inclusion trail patterns such as snowball garnets. We believe that there are two reasons for this. First, the problem is inherently complex and, as we show in this paper, except for near-spherical porphyroblasts, the three-dimensional (3D) geometry of inclusion trails is expected to be extremely complex. Second, misuse of reference frames, kinematic misconceptions, and violation of mechanical principles in some studies have added further confusion.

Many garnet porphyroblasts are approximately spherical, rendering their inclusion trails relatively interpretable. However, even for spherical garnets, unambiguous interpretation is commonly difficult. For example, simple sigmoidal inclusion trails with curvature less than 90° may be due to syntectonic rotation of the garnet relative to the foliation or due to post- or inter-tectonic helicitic growth over a crenulated foliation. It is not always possible to distinguish the different origins (e.g. Schoneveld, 1979). Slight differences in inclusion trail morphology may allow recognition of helicitic garnets (Schoneveld, 1979) and correlatable variation in the inclusion trajectory with hosting folds (e.g. Fyson, 1980) is good evidence of syntectonic relative rotation during folding (Jiang, 2001). The least ambiguous inclusion trails in garnets are, in our opinion, those of snowball garnets (with inclusion trails that curve much more than 90° from the center to the rim, e.g. Spry, 1963, 1969, p. 253; Schoneveld, 1979; Williams and Jiang, 1999) for they must be syntectonic, and following Schmidt (1918), Spry (1963, 1969), Schoneveld (1979) and many others, they have a simple explanation—recording the relative rotation between the garnet and the foliation in a non-coaxial progressive deformation history. However, Bell and co-workers have disputed this interpretation (e.g. Bell and Johnson, 1989; Bell et al., 1992a). They have proposed alternative models based on the notion that the garnets do not rotate with respect to the earth. Numerous papers have been published on the topic since Bell and Johnson (1989).

* Corresponding author. Present address: Department of Earth Sciences, University of Western Ontario, London ON, Canada N6A 5B7
E-mail address: dzjiang@geol.umd.edu (D. Jiang).

0191-8141/$ - see front matter © 2004 Elsevier Ltd. All rights reserved.
doi:10.1016/j.jsg.2004.06.012

Johnson (1993b) suggests that both the Schmidt–Schoneveld model and the models of Bell and co-workers may explain observations equally well (Johnson, 1993b, 1999), which, if true, would imply that the whole dispute is metaphysical. We do not repeat arguments already presented in the literature; interested readers may refer to the original papers (such as Bell and Johnson, 1989; Bell et al., 1992a,b; Passchier et al., 1992; Johnson, 1993a,b, 1999; Williams and Jiang, 1999) for details. The purposes of the present paper are instead: (1) to show that the 3D inclusion trails expected from elongate syntectonic porphyroblasts are too complex to be interpretable, (2) to clarify some confusion due to misuse of reference frames and misconceptions regarding kinematics in the literature, (3) to argue on a geometrical and kinematic basis that neither the original model of Bell and Johnson (1989) nor its modified form (Johnson, 1993b) for snowball garnet formation can be generally applicable, and (4) to demonstrate that the notion that rigid porphyroblasts in a deforming ductile matrix generally do not rotate with respect to the earth (or any other inertial frame) is unsound because it violates the fundamental physical law of the balance of angular momentum.

2. Complexity of inclusion trails from syntectonically-grown, elongate porphyroblasts

Rotation of a rigid object in 3D space has two effects. First, it reorients the object continuously. The orientation of an orthorhombic rigid body is defined by the plunge directions and plunge angles of its three symmetric axes, $\mathbf{a}_1$, $\mathbf{a}_2$, and $\mathbf{a}_3$ (Fig. 1a). Because the three axes are mutually perpendicular, three independent variables are sufficient to completely define the orientation of the object, such as plunge direction and plunge angle of one axis plus the plunge direction of a second axis. In the special case of one axis being horizontal, the three independent variables can be the azimuth of the horizontal axis plus the plunge direction and the plunge angle of a second axis. Rotation of the object leads to variation with time of the plunge directions and plunge angles of the symmetric axes. This may result in a preferred orientation fabric (Ježek et al., 1994, 1996) for a large population of elongate rigid objects.

The second effect of rotation is the rotation of the rigid object around its own symmetrical axes. The accumulation of this rotation over time, which we call *revolution* in this paper, gives rise to various inclusion trails in syntectonic porphyroblasts overgrowing a preexisting foliation.

The two effects of rotation are described mathematically in the following.

In the rigid body internal coordinate system defined by the symmetrical axes of the rigid object (the $a_1a_2a_3$ system shown in Fig. 1a), the angular velocity of a rigid object at an instant is:

$$\boldsymbol{\omega}' = \omega_1'\mathbf{a}_1 + \omega_2'\mathbf{a}_2 + \omega_3'\mathbf{a}_3 \tag{1}$$

where $\mathbf{a}_1$, $\mathbf{a}_2$, and $\mathbf{a}_3$ are unit vectors parallel to the respective axes.

Suppose $\mathbf{Q}$ is the coordinate transformation matrix from an external coordinate system $X_1X_2X_3$ (Fig. 1a) to the rigid body internal system. $\mathbf{Q}$ then relates the coordinates of a position vector in the external system (x_1, x_2, x_3) to its coordinates (x_1', x_2', x_3') in the rigid body internal system by:

$$\begin{pmatrix} x_1' \\ x_2' \\ x_2' \end{pmatrix} = \mathbf{Q}\begin{pmatrix} x_1 \\ x_2 \\ x_3 \end{pmatrix} \tag{2}$$

The instantaneous rotation of the rigid body in the external coordinate system is described by its angular velocity stated in the $X_1X_2X_3$ system:

$$\boldsymbol{\omega} = \mathbf{Q}^{\mathrm{T}}\boldsymbol{\omega}' \tag{3}$$

where $\mathbf{Q}^{\mathrm{T}}$ is the transposed matrix of $\mathbf{Q}$.

The first effect of rotation—reorienting of the three axes of the object—is described by the following equation:

$$\frac{\mathrm{d}\mathbf{a}_i}{\mathrm{d}t} = \boldsymbol{\omega} \times \mathbf{a}_i \quad (i = 1, \quad 2, \quad 3) \tag{4}$$

The second effect of rotation, revolution of the rigid body, is described by the accumulated rotation (Ω)—the time integral of the angular velocity around each axis:

$$\Omega_i = \int_0^t \omega_i' \mathrm{d}t \quad (i = 1, \quad 2, \quad 3) \tag{5}$$

Eq. (4) can be solved numerically, if the instantaneous angular velocity is computed from the theory of Jeffery (1922). A MathCad (Mathsoft Engineering and Education, Inc., http://www.mathsoft.com) program, CLASTRGD, is developed for numerical modeling of rigid clast rotation in ductile flows based on Jeffery's (1922) theory. The algorithm and program will be published separately. Fig. 1b–d presents rotation trajectories, up to a bulk shear strain of 25, of a triaxial ellipsoid (aspect ratio a_1:a_2:a_3 = 3:2:1) in a simple shear flow using CLASTRGD. The shear plane is north–south and vertical, the shear direction is horizontal, and the sense of shear is sinistral. The initial orientation of the ellipsoid is as follows: a_1-axis plunges 60°, 090°, a_2-axis plunges 0°, 180°, and a_3-axis plunges 30°, 270°. Fig. 1e presents the revolutions of the ellipsoid around its three

Fig. 1. Two effects of rigid object rotation: reorienting and revolution. (a) The orientation of a rigid object is defined by the trends and plunges of any three mutually perpendicular axes, such as the three symmetrical axes for an orthorhombic object shown here. Only three independent parameters are needed (such as trend θ and plunge ϕ of a_1-axis plus a trend of another axis). (b)–(d) Variation with time of the orientations of the long, intermediate, and short axes of a triaxial ellipsoidal object (aspect ratio of 3:2:1) embedded in a steady simple shear flow. Dashed arrow indicates upper hemisphere and solid arrows lower hemisphere equal-area projection. (e) Accumulated revolutions for the axes as the simple shear strain increase to 25. See text for details.

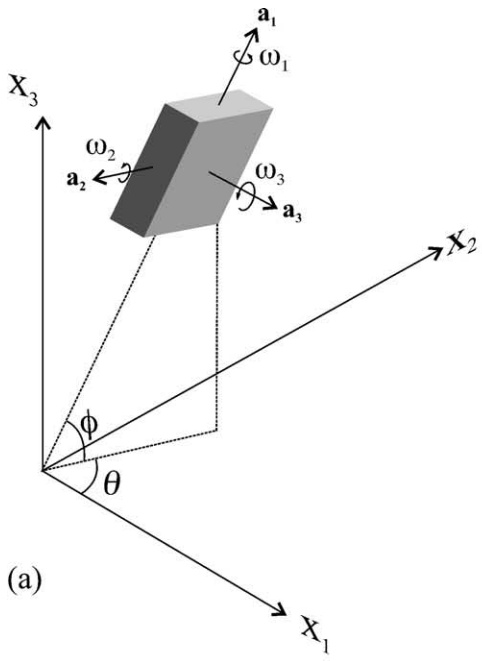
a1
ω1
X3
ω2
a2
ω3
a3
X2
ϕ
θ
X1

(a)

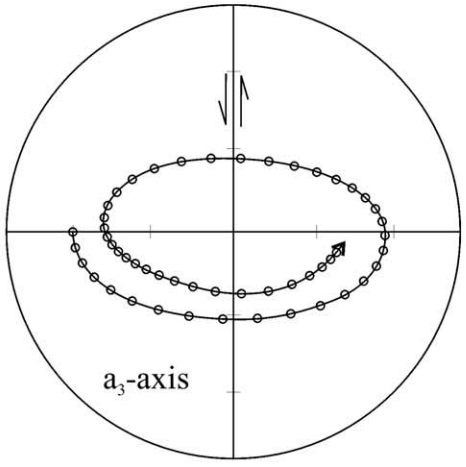
a3-axis

(d)

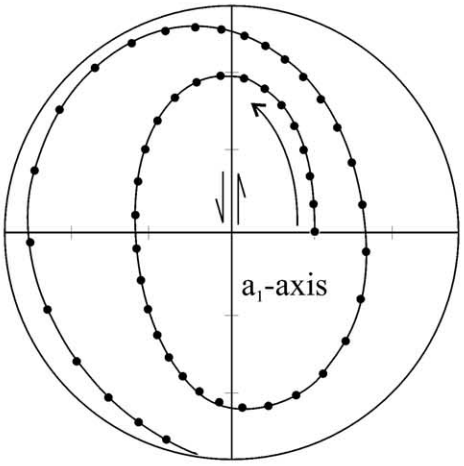
a1-axis

(b)

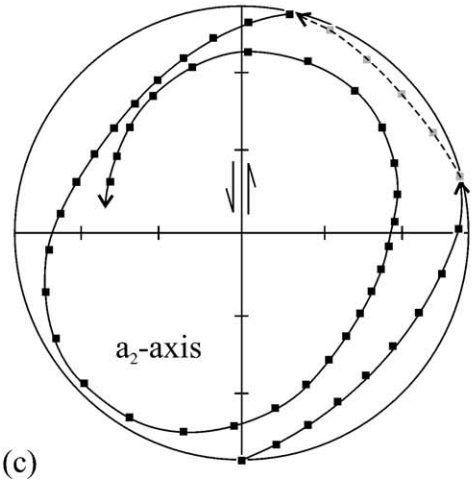
a2-axis

(c)

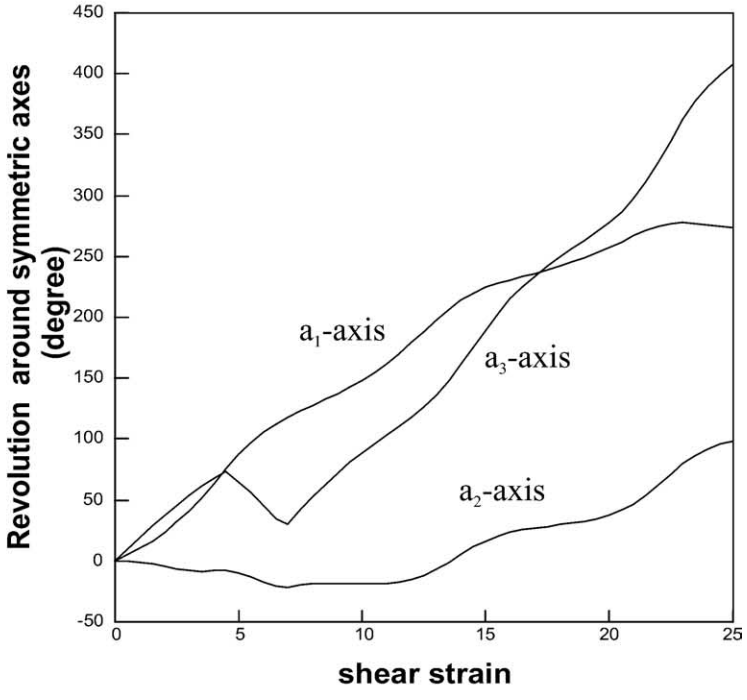
Revolution around symmetric axes (degree)
450
400
350
300
250
200
150
100
50
0
-50
0
5
10
15
20
25
shear strain
a1-axis
a3-axis
a2-axis

(e)

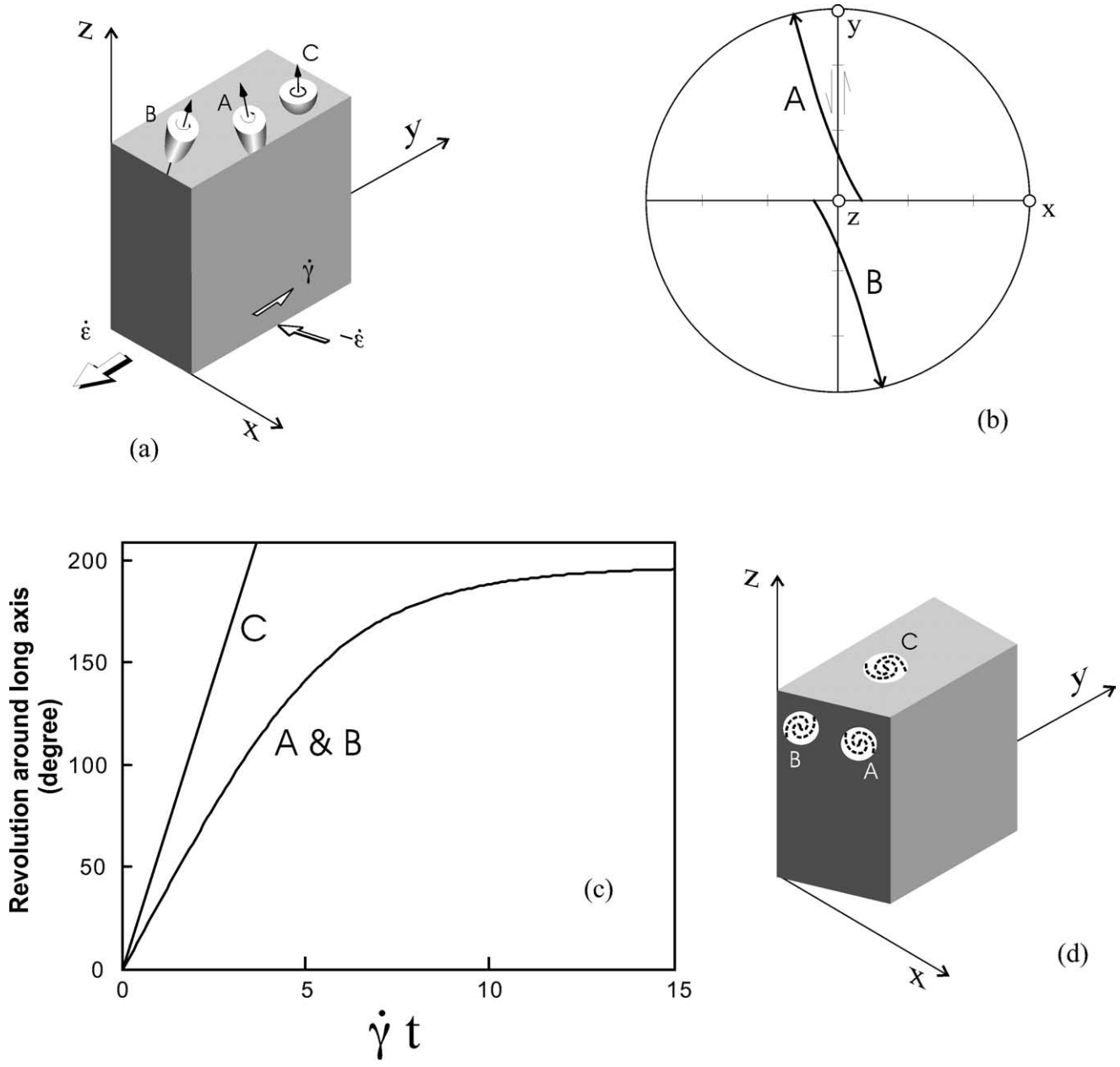

Fig. 2. Rotation and inclusion trail development in porphyroblasts of different initial shapes and orientations. (a) The flow described in a coordinate system *xyz*. The kinematic vorticity number is 0.5. Three rigid porphyroblasts A, B, and C are shown. C is spherical. A and B are spheroids with the same aspect ratio of 2:1:1. The initial plunge of A is 80°, 090°, and that of B is 80°, 270°. (b) The paths of the long axes for A and B (lower hemisphere equal-area projection). Both porphyroblasts reach the stable orientation making a synthetic angle of ~13° with the shear plane. (c) The accumulated spin around the symmetrical axes of the three porphyroclasts as the deformation advances. The horizontal axis is time multiplied by the shear strain rate. (d) The final senses of the spiral trails of porphyroblasts A and B are opposite and their long axes lie in the plane perpendicular to the vorticity and are ~13° synthetic to the *y*-axis (b). Porphyroblast C has inclusion trail sense the same as the vorticity and the trail axis is parallel to the vorticity. See text for more details.

respective axes calculated from numerical solution of Eq. (5).

One can appreciate the expected complexity of 3D inclusion trails in such an elongate porphyroblast even though the flow is simply a steady simple shear. For a spherical object, the rotation axis is always parallel to the vorticity vector of the surrounding fluid and, in a steady flow case, continues to be attached to the same material line of the object throughout. In distinction, the instantaneous angular velocity of a triaxial object ω is in general not parallel to any of its symmetrical axes and it varies with time (Jeffery, 1922). Thus, the revolution history of a non-spherical object depends on its initial orientation in the flow, its shape, and the flow kinematics. A small difference in initial orientation and/or shape can result in drastically different final inclusion trail geometries. Fig. 2 shows results

of another numerical example using CLASTRGD to illustrate this point. Consider a plane-strain deformation (Ramberg, 1975) with a kinematic vorticity number of 0.5 and with three porphyroblasts (A, B, and C) embedded in the flow. Porphyroblasts A and B are spheroidal with the same aspect ratio (2:1:1) but have slightly different initial orientations with A initially plunging 80°, east, and B initially plunging 80°, west. Porphyroblast C is spherical. For simplicity let us assume that the aspect ratios of the porphyroblasts do not change during growth. Fig. 2b shows the orientation trajectories of the long axes of A and B. Both porphyroblasts rotate to a stable orientation with the long axes making synthetic angles of 13° with respect to the shear zone boundary as predicted by the Jeffery theory (Passchier, 1987; Ježek et al., 1996). Both have undergone the same amount of revolution around their respective long axes because of their identical shape and symmetrical initial orientations with respect to the shear zone (Fig. 2c). However, the spiral axes of the inclusion trails are perpendicular, rather than parallel, to the flow vorticity, and the spirals have opposite senses of curvature on the section perpendicular to their long axes (Fig. 2d). Clearly the 3D inclusion trails of A and B do not have monoclinic symmetry. Ghosh et al. (2003) make similar observations for elongate clasts initially lying on the shear plane of the bulk flow. Porphyroblast C, being spherical, has the simplest inclusion trail with the spiral having the same sense as the flow vorticity and spiral axis parallel to the vorticity vector (z-axis, Fig. 2).

The above two numerical experiments serve to demonstrate that inclusion trails in elongate syntectonic porphyroblasts are extremely complex even for simple deformation histories (steady progressive simple shear) and simple porphyroblast shapes (spheroidal). We conclude that it is not possible to interpret 3D inclusion trails in elongate porphyroblasts in general. Interpretation of such porphyroblast inclusion trails should be regarded with suspicion and analyzed critically. However, preferred orientation fabrics defined by the principal axes of a population of elongate objects are more tractable.

3. Reference frame and the controversy regarding the formation of snowball garnet inclusion trails

The formation of snowball garnets was explained many years ago (Schmidt, 1918) by the rotation of garnets with respect to a foliation being overgrown by the garnets. Schoneveld (1979) designed a simple analogue model (Fig. 3) to demonstrate the process. The model has been elaborated by a number of authors using numerical modeling based on fluid dynamics (e.g. Masuda and Ando, 1988; Masuda and Mochizuki, 1989; Bjornerud and Zhang, 1994; Gray and Busa, 1994), but the idea remains the same. It can be summarized as follows in precise terms of the kinematics of continuum deformation: In a progressive deformation, the foliation behaves essentially like a material plane that rotates[1] toward a stable orientation (the major principal strain plane for a coaxial progressive deformation or the shear plane for a non-coaxial progressive deformation), but the garnet, being a small rigid body, rotates in response to the flow vorticity, if it is spherical, or both the flow vorticity and strain rates, if it is non-spherical. The difference in the angular velocities between the garnet and foliation as well as the history of garnet growth gives rise to the final inclusion trail geometry.

It is critical to realize that in the Schmidt–Schoneveld model it is the *relative* rotation (difference in angular velocity) between garnet and foliation that produces the inclusion trail curvature; whether there is absolute rotation of the garnet with respect to the earth is irrelevant. Using Schoneveld's simple analogue (the brass rings for the growing garnet and the strings for the foliation), all the following three statements describe the Schmidt–Schoneveld model and are equivalent:

Statement 1: The snowball pattern results from progressive rotation of the growing garnet with respect to the foliation.

Statement 2: The snowball pattern results from progressive rotation of the foliation with respect to the garnet.

Statement 3: The snowball pattern results from relative rotation between the garnet and the foliation.

The only difference between these statements lies in the implied reference frames used to describe the phenomenon. In statement 1, the reference frame is the foliation, in statement 2 it is the garnet, and in statement 3 an external reference frame such as the earth is used.

Bell and Johnson (1989) propose a strain partitioning model (SPM), in which the garnet overgrows *multiple-generations* of nearly orthogonal foliations (Fig. 4). This model differs fundamentally from the Schmidt–Schoneveld model in that in the latter *a single foliation* is overgrown by the garnet. It is this difference between the two models that gives rise to the distinctive 3D inclusion trail geometries predicted by the two models (Williams and Jiang, 1999). Williams and Jiang (1999) conclude that the 3D inclusion trail geometries can thus be used to discriminate the two models. They also point out that where the 3D geometry is documented, all naturally occurring snowball garnets, reported in the literature, are consistent with the predictions of the Schmidt–Schoneveld model but not with the SPM.

Because the SPM has in it the general notion that the garnet does not rotate relative to the earth, it has been frequently called the 'non-rotational model' (e.g. Johnson,

[1] The foliation as a material plane is generally stretched as well during deformation. But it is the rotation that is relevant here.

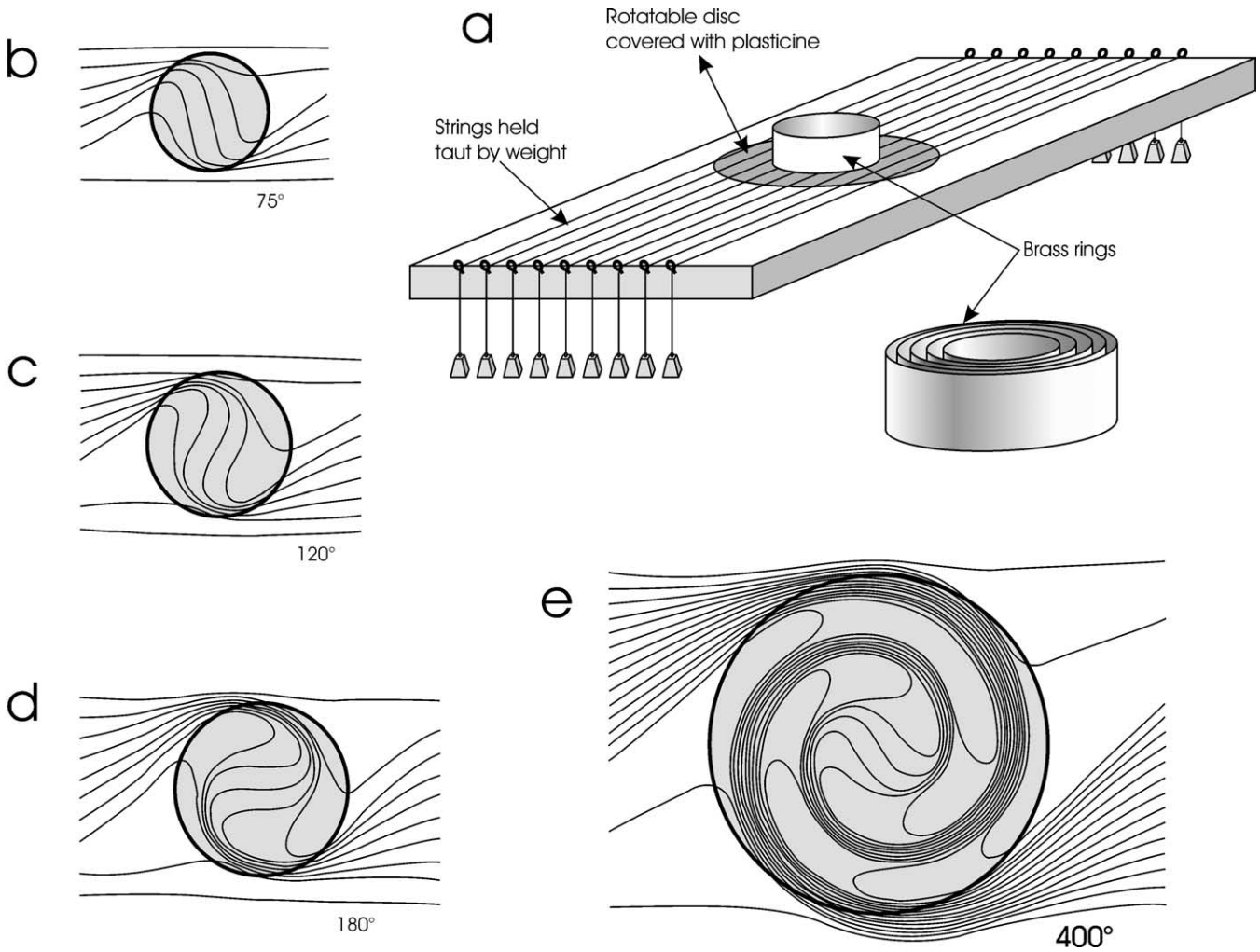

Fig. 3. The analogue model of Schoneveld (1979) demonstrating the formation of snowball garnets by the Schmidt–Schoneveld method. (a) Apparatus comprising a wooden board with a circular cut-out disc that is covered with plastine and can be rotated in the hole. Strings are stretched across the board and held taut by weights. Nesting brass rings are pressed into the plastine, concentric with the disc, starting with the smallest ring. After placement of each ring, the plastine-covered disc is rotated a given amount with respect to the wooden board. The rings pin the strings that they intersect to the disc, so that the segments of the strings within the rings are rotated with the disc. The strings represent the foliation and the rings represent successive garnet growth. The strings within the rings represent 'foliation inclusion trails' encapsulated within the 'garnet'. (b)–(e) Images traced from photos of the analogue experiment at different stages (total amount of rotation shown below each image). The strings in the actual model have straight-line segments between rings, but the lines have been smoothed in the diagram to represent continuous rather than stepwise growth. It is readily seen from this simple analogue that it makes no difference, for the final inclusion pattern, whether the wooden board was kept fixed to the earth and the disc was progressively rotated (clockwise here) (an easier experiment), or the disc was kept fixed and the wooden board was made to rotate progressively (anticlockwise) (a more inconvenient experiment). After Schoneveld (1979).

1993a,b; Passchier and Trouw, 1996; Williams and Jiang, 1999). This should not be confused with the statement 2 representation of the Schmidt–Schoneveld model; stating the Schmidt–Schoneveld model in the garnet reference frame (statement 2) does not make it the SPM.

Williams and Jiang (1999) did not propose that rotating a foliation around an irrotational (to earth) garnet would produce 3D inclusion geometries different from those produced by rotating the garnet with respect to the foliation (cf. Johnson, 1999; Stallard et al., 2002). We did argue that the former was an unlikely process for the formation of natural snowball garnets. Our stated reason for this was not that it would produce different inclusion trail geometries, but that the deformation paths associated with it are unlikely to occur in crustal deformation. We will return to this point in the next section.

Stallard et al. (2002) set out to use a numerical modeling approach to show that the 'non-rotational model' produces inclusion trail morphology very similar to the Schmidt–Schoneveld model, and conclude that 3D inclusion trail geometry cannot be used to distinguish between different models. However, the 'non-rotational model' modeled by them is not the SPM. Rather, it is simply the Schmidt–Schoneveld model stated in the garnet reference frame. Thus, their modeling has demonstrated the trivial point that statements 1 and 2 are equivalent. Stallard et al. (2002)

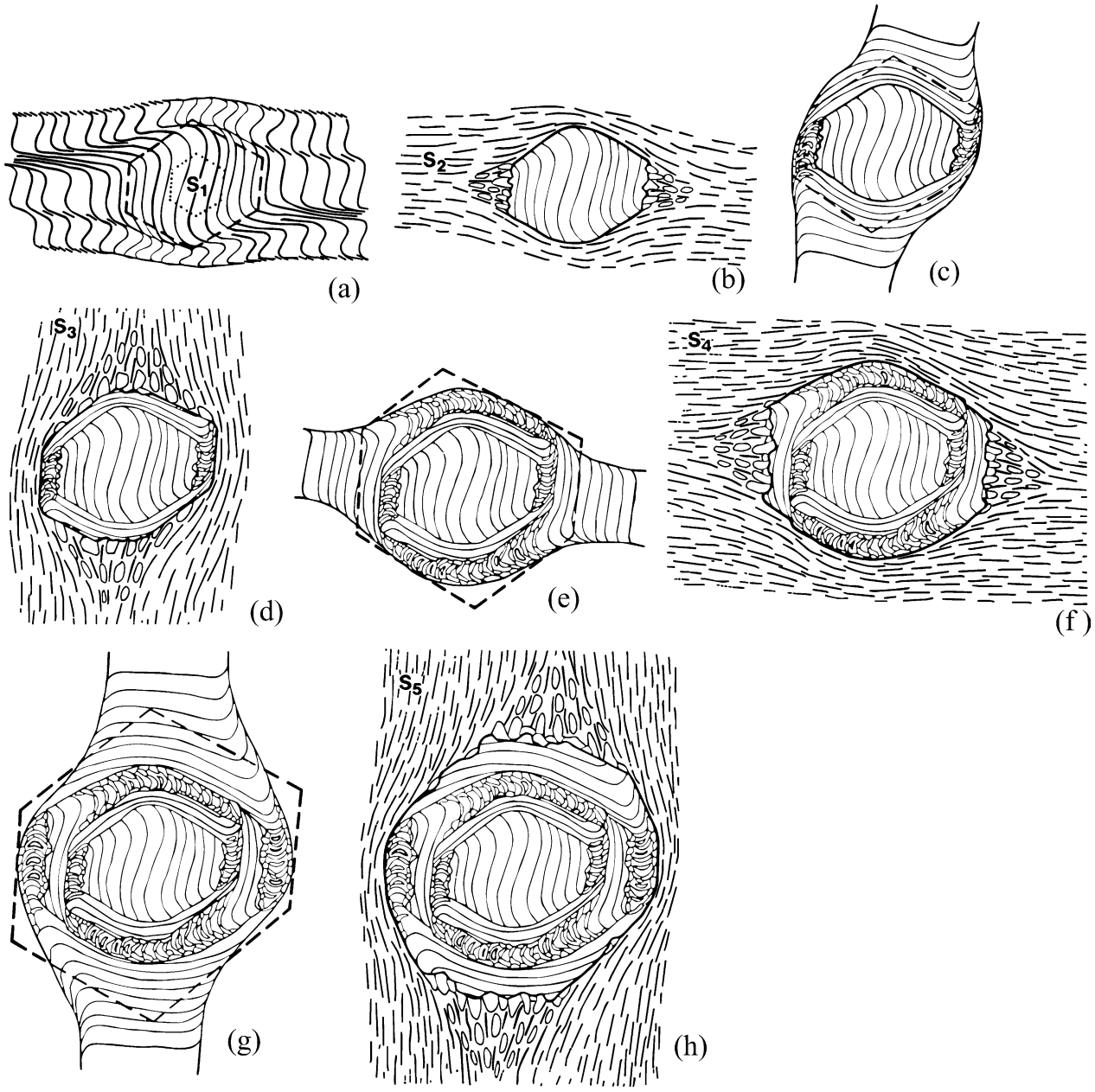

Fig. 4. The strain-partitioning model (SPM) of Bell and Johnson (1989) for the formation of snowball garnets, taken from Johnson (1993b). In this model the inclusion trails represent relicts of multi-generations of nearly orthogonal foliations [five generations (S_1–S_5) shown here]. The fundamental difference between this model and the Schmidt–Schoneveld model lies in the fact that in the SPM the garnet overgrows multiple generations of foliations whereas in the Schmidt–Schoneveld model (Fig. 1) a single foliation is overgrown by the garnet. Stating the Schmidt–Schoneveld model in the garnet reference frame does not make it the SPM.

report some minor differences in the inclusion geometry between their rotational and non-rotational sets of simulations. This can be readily explained by the fact that the two simulations actually represent dynamically different systems. In the rotational simulation, the rigid inclusion is subjected to the torque exerted by the surrounding fluid and it rotates in response to the vorticity to eliminate the torque. In their non-rotational simulation, the inclusion is held irrotational by an unspecified external torque to counteract the torque exerted by the surrounding fluid. We cannot imagine any source of such external torques in natural deformation.

4. The kinematic consequence of forming snowball garnets with the garnets irrotational with respect to the earth

Sharp curvature and truncation of inclusion trails are common in snowball garnets and they are explained in the

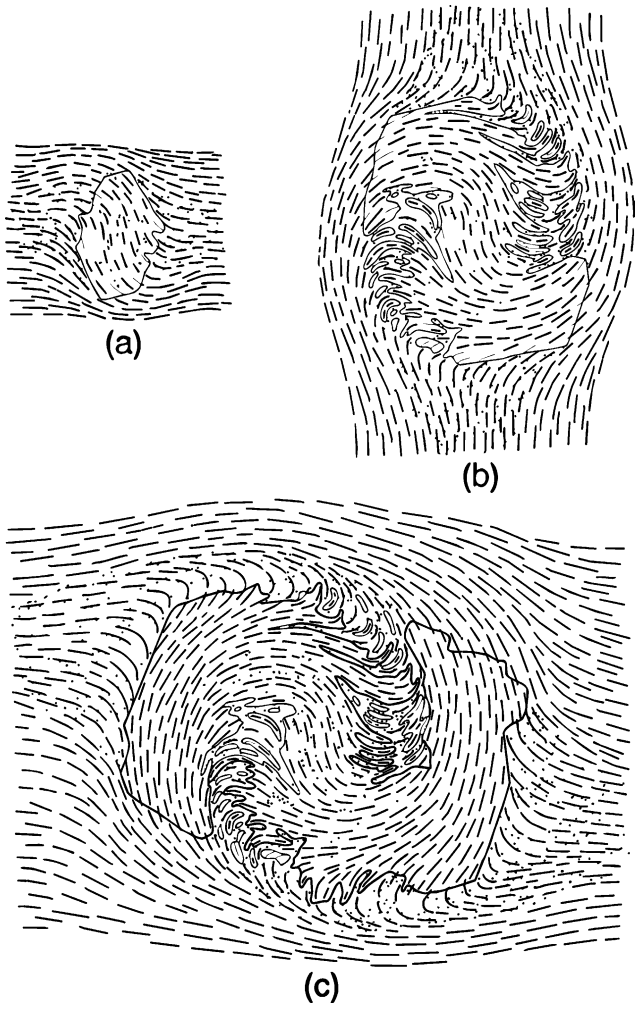

Fig. 5. Model presented by Johnson (1993b, fig. 9) and Johnson (1999) as a modification of the original SPM to explain the formation of continuous spirals in snowball garnet without garnet rotation (relative to earth). Supposedly, the modification is simply that successive foliations change smoothly and continuously from one to the other. However, the foliation being overgrown means it is no longer a crenulation cleavage comprising microlithons and septa, but is a penetrative foliation. Whether it is a single foliation or, as Johnson (1993b) suggests, smoothly and continuously connected successive segments of multi-generations of foliations that the garnet overgrows is irrelevant since as described, and shown, the successive foliations do not show overprinting. There is simply a gradual transition from one foliation to the other with a constant anticlockwise relationship between the new and the old. This situation is indistinguishable from a single foliation being wrapped around a garnet. It is therefore identical to the Schmidt–Schoneveld model, stated in the garnet reference frame (statement 2). See text for details. After Johnson (1993b).

Schmidt–Schoneveld model by periods of fast rate of rotation relative to rate of growth. The discontinuities are inherent in the SPM representing overprinting of successive nearly-orthogonal foliations. Natural snowball garnet trails, however, can be continuous, which is not compatible with the SPM. Johnson (1993a,b) presents some of the best examples of such continuous inclusion trails. He, following Bell et al. (1992a), provides an explanation (Johnson, 1993b, fig. 9) of how such continuous trails can form without garnet rotation relative to the earth (Fig. 5). He wrote: smoothly-curving snowball trails "may also imply that strain in the matrix surrounding a porphyroblast is relatively homogeneously distributed during successively overprinting deformation" (Johnson, 1993b, p. 640). He re-emphasized (Johnson, 1999, p. 1717) the idea of more distributed strain near the porphyroblast margins and claimed that the idea was already in the model of Bell and Johnson (1989): "The original non-rotational model presented by Bell and Johnson (1989) requires the developing foliation/crenulation cleavage to begin wrapping around the porphyroblast at an early stage of its growth, owing to heterogeneous shortening, rather than remaining planar throughout the entire growth phase as assumed by Williams and Jiang (1999)". The remarkable continuity of the foliation traces in Fig. 5 clearly suggests that a single foliation was overgrown by the garnet. If the trail in Fig. 5 does represent multiple generations of foliations, as Johnson claimed in the original figure caption (Johnson, 1993b, fig. 9) and in his recent review of the present paper, then successive foliations must be consistently anticlockwise to one another and the angle between them must be so small that they join so remarkably smoothly that they resemble a single foliation. Either way, a completely different deformation path from the original SPM is required as explained below.

Let us now look beyond a single garnet to see the kinematic consequence of forming snowball inclusion trails by the foliation (whether a single foliation, or successive segments of multi-generations of foliations joined smoothly) rotating and wrapping around an irrotational (to earth) garnet. As Fig. 6 shows, an observer on any garnet (say, garnet A) would find that the surrounding matrix material and garnets (B–G) are moving in circular paths. To produce a 360° inclusion curvature, the garnets must complete a circular revolution. If deformation paths such as this occur in nature, they will produce snowball garnets that are indistinguishable from snowball garnets from shear zones. But what environments can produce the required circular paths? One possibility is a special vortex (Truesdell, 1977, p. 99; Triton, 1988, p. 82–84) in which the particles move in circular paths around the vortex axis with the angular velocity (ω) inversely proportional to the square of the particle distance (r) from the vortex axis, i.e. $\omega = K/r^2$, where K is a constant (Fig. 7i). In such a vortex, a straight segment of a material line (initial trajectory of a 'foliation' in Fig. 7i), is changed to a spiral-shaped curve as flow advances. Initial small rigid inclusions ('garnets' a, b, c, …, g) move along circular paths to their new positions (A, B, C, …, G), but the orientation of each 'garnet' is unchanged because this is an irrotational (yet non-coaxial) flow (Lister and Williams, 1983; Triton, 1988, p. 82–84). Snowball trails are produced because of *relative* rotation of the 'foliation' with respect to the irrotational 'garnets' (Fig. 7ii). Another possible environment we can imagine is in convection cells where the material transport and velocity gradient

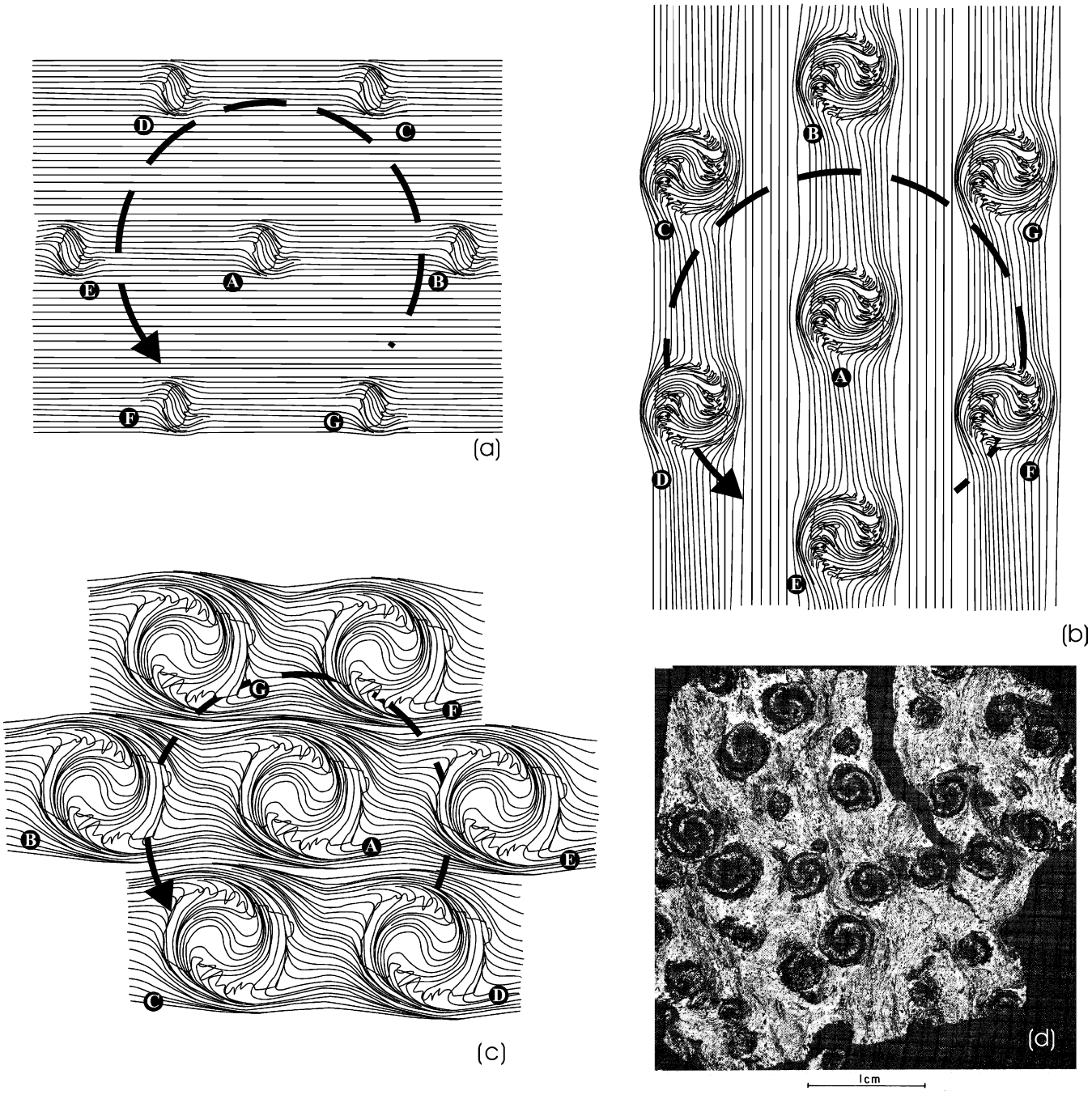

Fig. 6. Kinematic consequence of forming snowball garnets by rotating and wrapping the foliation around an irrotational-to-earth garnet. Parts (a)–(c) show different stages of this process. The particles around any garnet, say garnet A, must follow circular paths. Only in special vortex or fine-tuned convection cells is this type of deformation path possible. (d) Natural snowball garnets from Rosenfeld (1968). The foliation is represented as continuous lines here. In general, it is stretched as well as rotated during deformation. The garnet sketch is after Johnson (1993b, fig. 9). See text for details.

fortuitously (not a necessary characteristic of any convective flow) generate an irrotational (to earth) flow. Neither environment is likely for metamorphic terranes where snowball garnets are developed. As stated above, Williams and Jiang (1999) rejected the proposal of forming snowball inclusion trails by rotating and wrapping the foliation around an irrotational (to earth) garnet based on the unlikelihood of the required deformation paths.

5. Balance of angular momentum and porphyroblast rotation

The preceding sections are based on geometrical and kinematic arguments. We show in this section that the notion of irrotational rigid porphyroblasts in a deforming ductile matrix is unsound because it violates the fundamental physical law of balance of angular momentum.

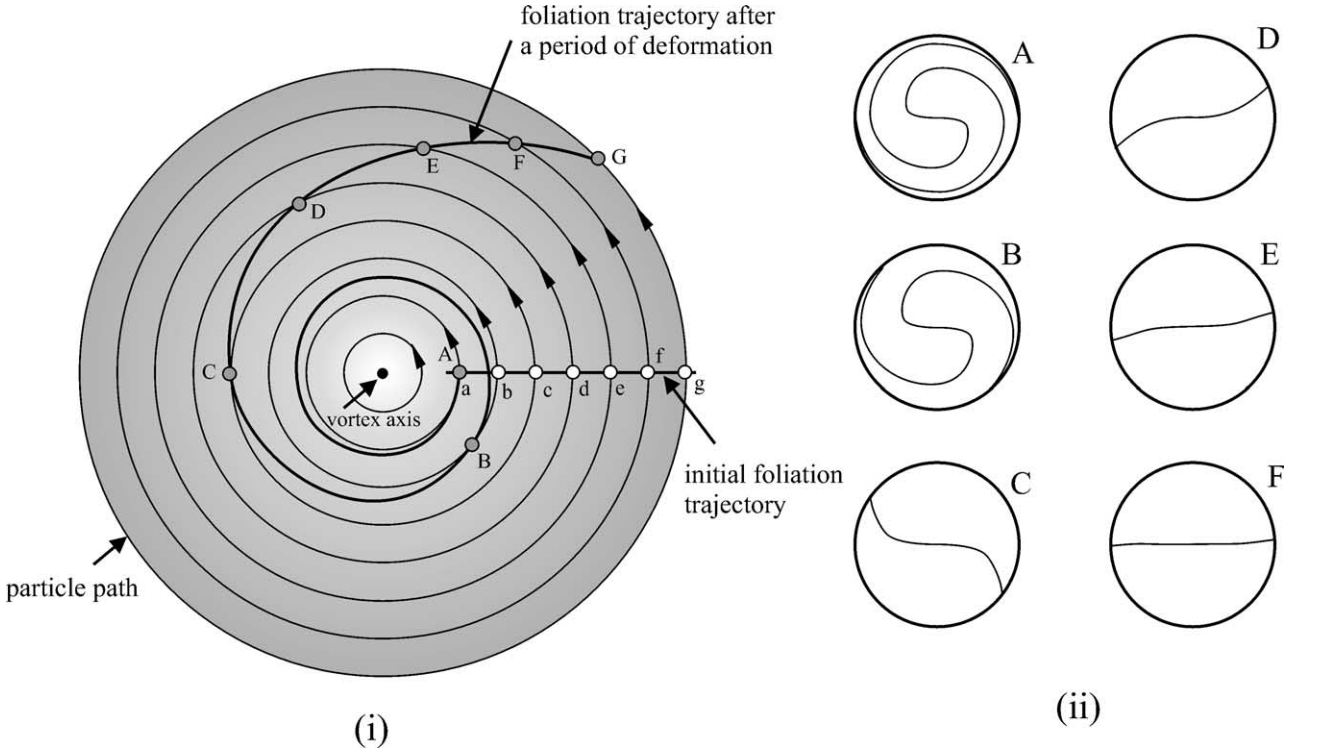

Fig. 7. Flow in a special vortex where the particles move on a circular path (an approximation of a real vortex in which particles have a slow radial velocity toward the vortex axis) and the angular velocity is inversely proportional to the square of the particle distance from the vortex axis. (i) Particle paths, distortion of a segment of material line representing foliation trace, and the initial and final positions of a few small rigid inclusions (a, b, c, …, g and A, B, C, …, G). Inclusion a (covered by A) has completed two revolutions. Although the 'garnets' move in circular paths, they do not change their own orientations because the flow is an irrotational (yet non-coaxial) one. (ii) Garnet inclusion trails expected of the 'garnets' as a result of relative rotation between the 'foliation' and 'garnets'. See text for more details.

For a rigid object, the law of balance of angular momentum (cf. MacMillan, 1936, p. 94) is stated mathematically as:

$$\boldsymbol{\tau} = \mathbf{I}\frac{\mathrm{d}\boldsymbol{\omega}}{\mathrm{d}t} \tag{6}$$

where $\boldsymbol{\tau}$ (a vector) is the total torque acting on the rigid object, $\mathbf{I}$ (a symmetrical rank 2 tensor) is the moment of inertia of the rigid object, and $\boldsymbol{\omega}$ (a vector), as in Fig. 1, is the angular velocity of the rigid object.

Eq. (6) is universal—it must be obeyed by motion of any rigid object. In the case of a spherical rigid object of uniform density, all three quantities in Eq. (6) are reduced to scalars and the moment of inertia is (cf. MacMillan, 1936, p. 40):

$$I = \frac{8}{15}\pi R^5 \rho \tag{7}$$

where R is the radius of the object and ρ is its density. Let us now consider balance of angular momentum for a few possible situations.

5.1. Situation 1: garnet in complete contact with the matrix

Where the garnet is in complete contact with the matrix (Fig. 8a), the total torque exerted on it by the deforming ductile matrix can be calculated using eq. (36) of Jeffery (1922):

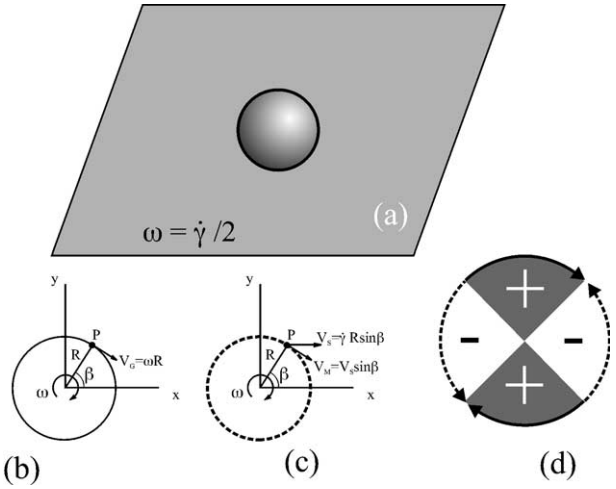

Fig. 8. The situation of garnet in complete contact with the matrix. (a) The garnet rotates at an angular velocity equal to half the vorticity. (b) The velocity (V_G) of an arbitrary point P on the surface of the garnet tangential to the surface. (c) The velocity (V_S) arising from the simple shear component of the flow at point P in the matrix. V_M is the tangential component of V_S. (d) Torque distribution on the surface of the garnet. Only a 2D section through the center of garnet is shown here which is sufficient for the analysis. See text for details.

$$\tau = \frac{16\pi\mu\left(\frac{w}{2}-\omega\right)}{3\alpha} \tag{8}$$

where μ is the matrix viscosity, w is the magnitude of the matrix vorticity, and α is defined by the following integral (Jeffery, 1922, p. 164):

$$\alpha = \int_0^\infty \frac{\mathrm{d}\lambda}{(R^2+\lambda)^{5/2}} = \frac{2}{3R^3} \tag{9}$$

Inserting Eq. (9) into Eq. (8), one obtains:

$$\tau = 8\pi\mu R^3\left(\frac{w}{2}-\omega\right) \tag{10}$$

In a slow motion, the balance of angular momentum requires that the torque vanish ($\tau=0$) at all times, which leads to the well-known relationship:

$$\omega = \frac{w}{2} = \frac{\dot{\gamma}}{2} \tag{11}$$

where $\dot{\gamma}$ is the simple shear strain rate parallel to the shear plane.

One can better understand this result by considering the traction distribution on the garnet surface (Fig. 8a). It is sufficient to consider the traction arising from the simple shear component only, because the pure shear component does not lead to a net torque. The tangential velocity of an arbitrary particle P (Fig. 8b) on the garnet surface is:

$$V_\mathrm{G} = \omega R \tag{12}$$

At point P, the matrix particle velocity resulting from the simple shear component of the flow in the same direction as V_G, if the garnet were not present, is (Fig. 8c):

$$V_\mathrm{M} = \dot{\gamma} R \sin^2\beta \tag{13}$$

In the sector $V_\mathrm{M} > V_\mathrm{G}$ the matrix exerts a positive torque on the garnet and in the sector $V_\mathrm{M} < V_\mathrm{G}$, the matrix exerts a negative torque. Varying β from 0 to 360°, i.e. taking the integral of $\int_0^{2\pi}(V_\mathrm{G}-V_\mathrm{M})\mathrm{d}\beta$ and setting it to zero, one finds that Eq. (11) is the only solution for the total torque to vanish (Fig. 8a).

Suppose now a porphyroblast was not rotating initially. Is it possible for it to remain irrotational? The answer is no, because of the requirement of the balance of angular momentum as explained below.

Inserting Eqs. (7) and (10) into Eq. (6), and after simplifying, the expression for the balance of angular momentum for a spherical object becomes:

$$\frac{\mathrm{d}\omega}{\mathrm{d}t} = \frac{15\mu}{R^2\rho}\left(\frac{w}{2}-\omega\right) \tag{14}$$

Solving Eq. (14) with the initial irrotational condition of $\omega|_{t=0} = 0$, we have:

$$\omega = \frac{w}{2}\left(1-\exp\left(-\frac{15\mu}{R^2\rho}t\right)\right) \tag{15}$$

A simple calculation using Eq. (15) with, say, a set of parameters of the following: $\mu = 10^{19}$ Pa s, $R = 0.01$ m, and $\rho = 3300$ kg/m^3 shows that it takes less than 10^{-19} s for ω to approach $w/2$! That is, the rigid object, irrotational initially, is driven to rotate at an angular velocity required by the matrix vorticity almost instantaneously.

5.2. Situation 2: garnet partially insulated from the matrix by a low-viscosity material

In some cases the garnet may be separated from the deforming matrix by a low-viscosity material, leading to what has been variably called ‘decoupling’, ‘incoherent contact’, or ‘interface slip’ between the garnet and the matrix (e.g. Mancktelow et al., 2002). Jeffery’s theory cannot be directly applied to this situation, but the angular momentum law still holds and the total torque acting on a garnet must vanish.

The presence of a low-viscosity material between the garnet and the matrix alters the traction distribution. The effect will differ with the location of the low-viscosity material. If it is in the sector of positive torque (top and bottom, Fig. 8d), the reduction in positive torque will cause the garnet angular velocity to decrease ($\mathrm{d}\omega/\mathrm{d}t < 0$) until the torque balance is reestablished and the garnet rotates at $\omega < w/2$. If the low viscosity material is located in the negative torque sector (Fig.8d), the garnet angular velocity will increase ($\mathrm{d}\omega/\mathrm{d}t > 0$) until the torque balance is reestablished. Fig. 9a shows a case where the low viscosity material is distributed evenly over the positive and negative torque sectors (Fig. 9b). The angular velocity will remain unchanged for this case.

If the garnet is completely isolated by a low viscosity mantle from the average matrix, then the vorticity in the matrix cannot be directly related to the angular velocity of the garnet. However, unless the low-viscosity mantle material is inviscid, it will transmit angular momentum from the matrix to the garnet, which drives the garnet to rotate. In porphyroclast systems (Passchier and Simpson, 1986), fine-grained dynamically recrystallized material derived from the shrinking porphyroclast may constitute a low-viscosity shell separating the clast from the matrix. Since garnet porphyroblasts grow, rather than shrink, and since the low-viscosity mantle is being deformed continually (Fig. 10), we do not think it likely that garnet porphyroblasts can be completely surrounded by a low-viscosity shell for geologically significant times.

5.3. Situation 3: garnet in point contact with the matrix (the ball-bearing case)

If the garnet is surrounded by a low-viscosity material but maintains in point contact with the matrix, the situation resembles the ball-bearing case (Fig. 9c and d). To balance the angular momentum, there must be no frictional force between the garnet and the matrix at the contact. This requires the garnet angular velocity to satisfy (Fig. 9e):

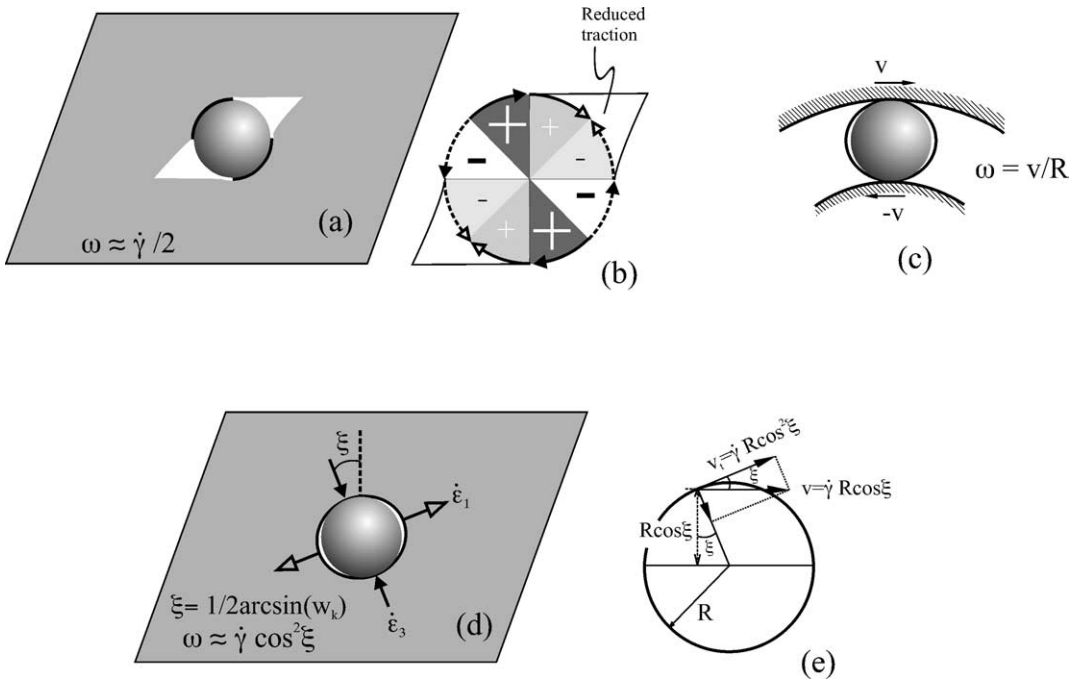

Fig. 9. The situations of garnet partially separated from the average matrix by a low viscosity material. (a) The presence of a pressure shadow (low viscosity material) may not change the torque balance because the shadow sectors evenly cover part of the sector of positive traction and part of sector of negative traction (b). (c) Ideal ball-bearing mechanism where the angular velocity of the ball is equal to the tangential velocity divided by the radius of the ball. (d) Ball-bearing-like mechanism may operate in nature at least transiently. If the location of the contact point between the matrix and the porphyroblast is determined by the orientation of the principal strain rates ($\dot{\varepsilon}_1$,$\dot{\varepsilon}_3$) the angular velocity of the porphyroblast can be related to the bulk vorticity number. (e) The garnet must rotate at an angular velocity equal to the tangential velocity at the contact point (V_t) divided by its radius. See text for details.

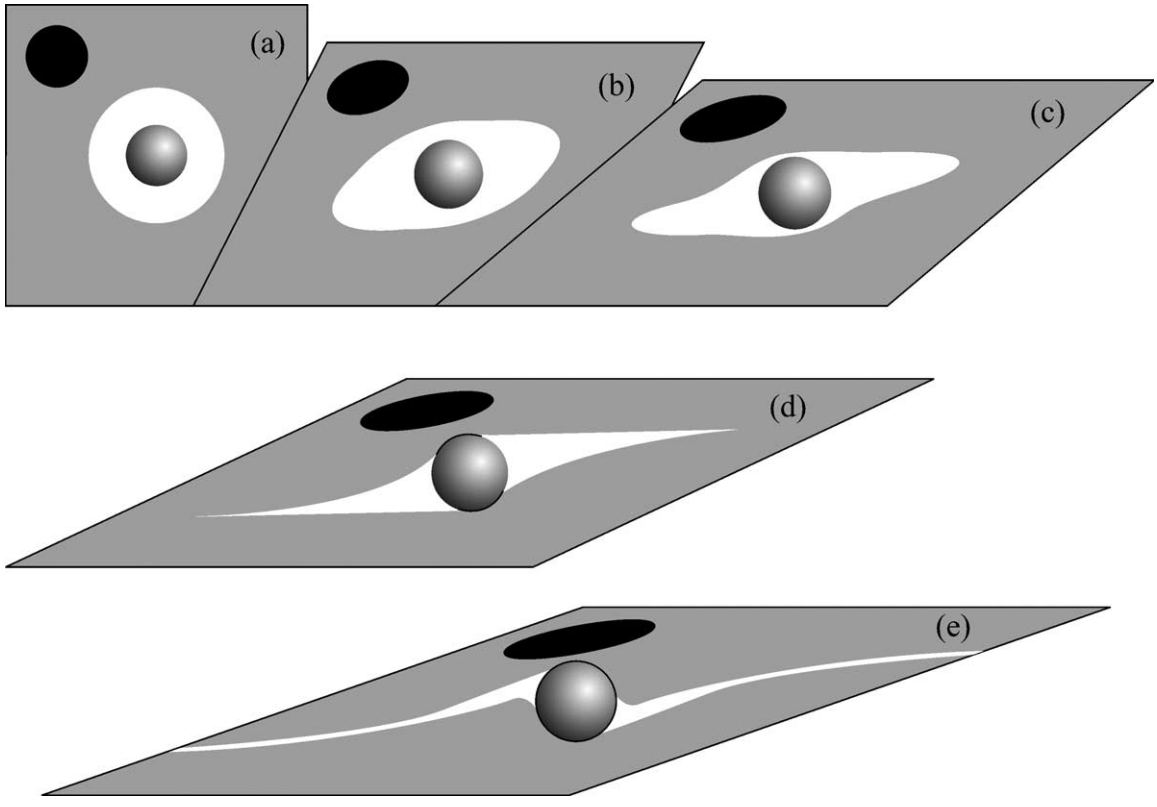

Fig. 10. Various situations that may occur at different stages of a snowball garnet formation. (a) and (b) Garnet completely insulated from the matrix by a low viscosity material. The garnet angular velocity cannot be simply related to the matrix vorticity. (c) Point contact between the matrix and the garnet (ball-bearing-like mechanism). (d) and (e) Garnet in partial to complete contact with the matrix. See text for discussion.

$$R\omega = \dot{\gamma} R \cos^2 \xi \tag{16}$$

which leads to:

$$\omega = \dot{\gamma} \cos^2 \xi \tag{17}$$

where ξ is the angle between the contact point orientation and the shear plane normal (Fig. 9d). For perfect spherical garnets, ξ can be related to the kinematic vorticity number, W_k, of the flow by (e.g. Jiang, 1994b):

$$\xi = \frac{1}{2} \sin^{-1} W_k \tag{18}$$

In a non-coaxial progressive deformation environment, syntectonically growing garnets may experience various situations at different stages of their development. Fig. 9 schematically illustrates this scenario.

6. Discussion

The various situations considered in the last section are based on the assumption of perfect spherical rigid garnets. Rotation of elongate and/or deformable objects in ductile flow is far more complicated. And the presence of low-viscosity material in the interface between the object and the matrix may affect the rotational behavior far more significantly (Mancktelow et al., 2002).

Strain localization is another issue affecting the rotational behavior of porphyroblasts. ten Grotenhuis et al. (2002) use a Mohr–Coulomb material (tapioca pearls) to investigate the influence of strain localization on the rotational behavior of mica-fish shaped rigid objects. They suggest that localized deformation may be common in the development of mylonites. From a kinematic point of view, the effect of localization is a highly heterogeneous distribution of the vorticity flux (Jiang, 1994a). If shear is highly localized into C-surfaces in a shear zone, then the C-surfaces take most of the vorticity flux leaving the domains between C-surfaces with far less vorticity. This may explain the stable orientation of elongate porphyroclasts such as micas. However, snowball garnets do not just grow in the domain between the C-foliations; they overgrow them. Localization on the scale smaller than the garnet porphyroblasts should not alter their rotational behavior.

The motion of porphyroblasts, irrespective of their shapes and the deformation conditions that they are subjected to, must all obey the law of balance of angular momentum. While it is certainly possible that in special cases a porphyroblast may have zero angular velocity, the notion that rigid objects embedded in a deforming ductile matrix are in general irrotational with respect to the earth violates the law of balance of angular momentum and should be abandoned.

7. Conclusions

The 3D inclusion trails of non-spherical syntectonic porphyroblasts are expected to be extremely complex. They do not generally have monoclinic symmetry even for the simplest deformation path. Each porphyroblast is a unique initial value problem depending on its initial orientation and shape. It is in general not possible to interpret such inclusion trails. However, shape preferred orientations defined by alignment of elongate porphyroblasts are interpretable.

The physics of a system does not change simply because one changes the reference frame used to describe it. Stating the Schmidt–Schoneveld model in the garnet reference frame does not make it the SPM.

The original SPM (not to be confused with statement 2 representation of the Schmidt–Schoneveld model) is not supported by evidence, because the 3D inclusion trail geometry that it predicts is not observed in naturally occurring snowball garnets reported so far. The modified form of it requires special deformation paths that are unlikely to occur in crustal deformation.

While the relationship between the rotation of rigid porphyroblasts and the matrix flow varies with the interface property, the notion that rigid inclusions in a deforming ductile matrix do not in general rotate violates the physical law of the balance of angular momentum and should be abandoned.

Acknowledgements

We thank Dr Cees Passchier for his comments on early drafts of the paper and sharing his yet unpublished material with us. We thank Dr Declan De Paor for review comments. The work is supported by NSF-EAR 0003315 and a Petroleum Research Fund to DJ and an NSERC Discovery Grant to PFW.

References

Bell, T.H., Johnson, S.E., 1989. Porphyroblast inclusion trails: the key to orogenesis. Journal of Metamorphic Geology 7, 279–310.

Bell, T.H., Forde, A., Hayward, N., 1992a. Can smoothly curved spiral-shaped inclusion trails form without rotation of the porphyroblast? Geology 20, 59–62.

Bell, T.H., Johnson, S.E., Davis, B., Forde, A., Hayward, N., Wilkins, C., 1992b. Porphyroblast inclusion-trail data: eppure non son girate! Journal of Metamorphic Geology 10, 295–307.

Bjornerud, M.G., Zhang, H., 1994. Rotation of porphyroblasts in non-coaxial deformation: insights from computer simulations. Journal of Metamorphic Geology 12, 135–139.

Fyson, W.K., 1980. Fold fabrics and emplacement of an Archean granitoid pluton, Cleft Lake, Northwest Territories. Canadian Journal of Earth Sciences 17, 325–332.

Ghosh, S.K., Sen, G., Sengupta, S., 2003. Rotation of long tectonic clasts in transpressional shear zones. Journal of Structural Geology 25, 1083–1096.

Gray, N.H., Busa, M.D., 1994. The three-dimensional geometry of simulated porphyroblast inclusion trails: inert-marker, viscous-flow models. Journal of Metamorphic Geology 12, 575–587.

ten Grotenhuis, S.M., Passchier, C.W., Bons, P.D., 2002. The influence of strain localization on the rotation behaviour of rigid objects in experimental shear zones. Journal of Structural Geology 24, 485–499.

Jeffery, G.B., 1922. The motion of ellipsoid particles immersed in a viscous fluid. Proceedings of the Royal Society of London, Series A 102, 161–179.

Ježek, J., Melka, R., Schulmann, K., Venera, Z., 1994. The behavior of rigid triaxial particles in viscous flows—modeling of fabric evolution in a multiparticle system. Tectonophysics 229, 165–180.

Ježek, J., Schulmann, K., Segeth, K., 1996. Fabric evolution of rigid inclusions during mixed coaxial and simple shear flows. Tectonophysics 257, 203–221.

Jiang, D., 1994a. Vorticity determination, distribution, and partitioning, and the heterogeneity and non-steadiness of natural deformations. Journal of Structural Geology 16, 121–130.

Jiang, D., 1994b. Flow variation in layered rocks subjected to bulk flow of various kinematic vorticities: theory and geological implications. Journal of Structural Geology 16, 1159–1172.

Jiang, D., 2001. Reading history of folding from porphyroblasts. Journal of Structural Geology 23, 1327–1335.

Johnson, S.E., 1993a. Unravelling the spiral: a serial thin-section study and three-dimensional computer-aided reconstruction of spiral-shaped inclusion trails in garnet porphyroblasts. Journal of Metamorphic Geology 11, 621–634.

Johnson, S.E., 1993b. Testing models for the development of spiral-shaped inclusion trails in garnet porphyroblasts: to rotate or not to rotate, that is the question? Journal of Metamorphic Geology 11, 635–659.

Johnson, S.E., 1999. Porphyroblast microstructures: a review of current and future trends. American Mineralogist 84, 1711–1726.

Lister, G.S., Williams, P.F., 1983. The partitioning of deformation in flowing rock masses. Tectonophysics 92, 1–33.

MacMillan, W.D., 1936. Dynamics of Rigid Bodies. McGraw-Hill, New York.

Mancktelow, N.S., Arbaret, L., Pennacchioni, G., 2002. Experimental observations on the effect of interface slip on rotation and stabilisation of rigid particles in simple shear and a comparison with natural mylonites. Journal of Structural Geology 24, 567–585.

Masuda, T., Ando, S., 1988. Viscous flow around a rigid spherical body: a hydrodynamical approach. Tectonophysics 148, 337–346.

Masuda, T., Mochizuki, S., 1989. Development of snowball structure: numerical simulation of inclusion trails during synkinematic porphyroblast growth in metamorphic rocks. Tectonophysics 170, 141–150.

Passchier, C.W., 1987. Stable positions of rigid objects in non-coaxial flow—a study in vorticity analysis. Journal of Structural Geology 9, 679–690.

Passchier, C.W., Simpson, C., 1986. Porphyroclast systems as kinematic indicators. Journal of Structural Geology 8, 831–844.

Passchier, C.W., Trouw, R.A.J., 1996. Microtectonics. Springer-Verlag, New York.

Passchier, C.W., Trouw, R.A.J., Zwart, H.J., Vissers, R.L.M., 1992. Porphyroblast rotation: eppur si muove? Journal of Metamorphic Geology 10, 283–294.

Ramberg, H., 1975. Particle paths, displacement and progressive strain applicable to rocks. Tectonophysics 28, 1–37.

Rosenfeld, J.L., 1968. Garnet rotations due to the major Paleozoic deformations in Southeast Vermont, in: Zen, E., White, W.S., Hadley, J.B., Thompson Jr., J.B. (Eds.), Studies of Appalachian Geology: Northern and Maritime. Interscience Publishers, New York, pp. 185–202.

Schmidt, W., 1918. Bewegungsspuren in Porphyroblasten Kristalliner Schiefer, Sitzungsber. Akademie der Wissenschaften in Wien, Mathematisch-Naturwissenschaften Klasse, Abteiling 1 (127), 293–310.

Schoneveld, C., 1979. The geometry and significance of inclusion patterns in syntectonic porphyroblasts. Published PhD thesis, University of Leiden, The Netherlands.

Spry, A., 1963. The origin and significance of snowball structure in garnet. Journal of Petrology 4, 211–222.

Spry, A., 1969. Metamorphic Textures. Pergamon Press, New York.

Stallard, A., Ikei, H., Masuda, T., 2002. Numerical simulations of spiral-shaped inclusion trails: can 3D geometry distinguish between end-member models of spiral formation? Journal of Metamorphic Geology 20, 801–812.

Triton, D.J., 1988. Physical Fluid Dynamics. Clarendon Press, Oxford.

Truesdell, C., 1977. A First Course in Rational Continuum Mechanics. Academic Press, New York.

Williams, P.F., Jiang, D., 1999. Rotating garnets. Journal of Metamorphic Geology 17, 367–378.